

CALCULATION OF DENSE SNOW AVALANCHES IN THREE-DIMENSIONAL TERRAIN WITH THE NUMERICAL SIMULATION PROGRAM RAMMS

Marc Christen*, Perry Bartelt, Julia Kowalski and Lukus Stoffel
WSL Institute for Snow and Avalanche Research SLF

ABSTRACT: Numerical models have become an essential part of snow avalanche engineering. Recent advances in understanding the rheology of flowing snow and the mechanics of entrainment and deposition have made numerical models more reliable. Coupled with field observations and historical records, they are especially helpful in understanding avalanche flow in complex terrain. However, the application of numerical models poses several new challenges to avalanche engineers. A detailed understanding of the avalanche phenomena is required to specify initial conditions (release zone dimensions and snowcover entrainment rates) as well as the friction parameters, which are no longer based on empirical back-calculations, rather terrain roughness, vegetation and snow properties. In this paper we discuss these problems by presenting the computer model RAMMS, which was specially designed by the SLF as a practical tool for avalanche engineers. RAMMS solves the depth-averaged equations governing avalanche flow with first and second-order numerical solution schemes. A tremendous effort has been invested in the implementation of advanced input and output features. Simulation results are therefore clearly and easily visualized to simplify their interpretation. More importantly, RAMMS has been applied to a series of well-documented avalanches to gauge model performance. In this paper we present the governing differential equations, highlight some of the input and output features of RAMMS and then discuss the simulation of the Gatschiefer avalanche that occurred in April 2008, near Klosters/Monbiel, Switzerland.

KEYWORDS: snow, avalanche, dynamics, modeling, numerical simulation, hazard mapping

1. INTRODUCTION

An accurate prediction of avalanche runout distances, flow velocities and impact pressures in general three-dimensional terrain is the driving motivation for the development of avalanche dynamics models. Presently, one-dimensional numerical models, such as AVAL-1D (Bartelt et al., 1999; Christen et al., 2002), are used extensively in Switzerland, Austria and Italy. Although helpful and well-liked by users, one-dimensional models require that the primary avalanche flow direction and flow width must be defined by the user in advance. This is often difficult, especially in open terrain, or in terrain consisting of several possible flow channels. Furthermore, avalanche interaction with catching and deflecting dams cannot be accurately modeled using one-dimensional simulation codes.

In this paper we will present the two-dimensional simulation model RAMMS, which was specifically designed to resolve the limitations of one-dimensional avalanche dynamics models. The model development is based on extensive chute experiments with flowing snow (Kern et al., 2004) and observations of real scale avalanches at the Swiss Vallée de la Sionne test site (Sovilla et al., 2006, 2007; Kern et al., 2008). The two primary results of this experimental work are (1) rate- and stress-based snowcover entrainment models (Sovilla et al., 2006, 2007) and (2) the formulation of an additional differential equation governing the generation, transport and decay of random kinetic energy in avalanches (Bartelt et al., 2005, 2006; Buser and Bartelt, 2008a,b). The improved model physics in RAMMS is supplemented with advanced second-order solution methods which ameliorate numerical diffusion (spreading) problems on open slopes.

* *Corresponding author address:* Marc Christen. WSL Institute for Snow and Avalanche Research, SLF, Department of Avalanches, Debris Flows and Rockfalls, Davos Dorf, Switzerland; phone: 0041-81-417-0106; email: christen@slf.ch

Above all, RAMMS was designed to be a helpful tool for avalanche engineers. A tremendous effort was invested in easy-to-use input features as well as advanced visualization of the numerical output (Christen et al., 2007).

In this paper we state the governing equations describing avalanche flow with entrainment in RAMMS, discuss their numerical solution and then apply the model to simulate a large, wet snow avalanche that occurred in April 2008 in Gatschiefer/Klosters, Switzerland (Fig. 1).



Figure 1: The Gatschiefer avalanche, Klosters, 23.4.2008. Picture shows release zone, avalanche track and deposition area. Note the avalanche flowed in several channels. An avalanche deflecting dam is located at the right of the beginning of the runout zone.

2. NUMERICAL MODEL

RAMMS numerically solves a system of partial differential equations, governing the depth-averaged balance laws for mass, momentum and random kinetic energy using first and second order finite volume techniques.

2.1 Governing Differential Equations

The computational domain is defined in two-coordinate directions x and y . The elevation of the terrain is given by $z(x, y)$ and is

typically obtained from a digital elevation model (DEM). The specification of the DEM will be explained in more detail in Section 3.

Let $H(x, y, t)$ be the flow height of the avalanche at time t ; $U_x(x, y, t)$ and $U_y(x, y, t)$ are the mean avalanche velocities in the x and y directions, respectively. The quantities

$$n_x = \frac{U_x}{\sqrt{U_x^2 + U_y^2}} \text{ and } n_y = \frac{U_y}{\sqrt{U_x^2 + U_y^2}} \quad (1)$$

define the cosine and sine of the flow direction of the avalanche in the x - y plane, respectively.

We denote the total mean avalanche velocity

$$U = \sqrt{U_x^2 + U_y^2}.$$

Mass balance is given by

$$\partial_t H + \partial_x (HU_x) + \partial_y (HU_y) = \dot{Q} \quad (2)$$

where $\dot{Q}(x, y, t)$ is the snow entrainment rate.

Let $l(x, y, t)$ be the length of the snowcover overrun by the avalanche, then

$$\dot{Q}(x, y, t) = \begin{cases} 0 & \text{if } h_i = 0 \\ \frac{\rho_i}{\rho_a} h_i \frac{U}{l} & \text{if } k_i l \geq h_i \\ \frac{\rho_i}{\rho_a} k_i U & \text{if } k_i l < h_i \end{cases} \quad (3)$$

where h_i is the height of the i -th snow layer;

ρ_i is the density of the i -th layer. The density of the avalanche is constant and denoted ρ_a . The

dimensionless parameter k_i defines the entrainment rate for a unit flow velocity. In RAMMS it is possible to define a maximum of three snow layers ($i \leq 3$), each with a different height, density and unit entrainment rate. We refer to this entrainment procedure as a *rate* or *mass-controlled* model since the parameter k_i controls the entrainment rate directly. This differs from a *stress-controlled* procedure where a limit stress determines the entrainment rate (Sovilla et al., 2005). We have found stress-controlled procedures to be somewhat artificial because the limit stress is arbitrarily chosen such that the measured entrainment rates are reached. With $0.05 \leq k_i \leq 0.5$ we have entrainment rates

between $100 \text{ kg/m}^2 \text{ s} \leq \rho_i \dot{Q} \leq 500 \text{ kg/m}^2 \text{ s}$, in good agreement with measurements at the Vallée de la Sionne test site (see Sovilla et al., 2006).

The momentum balance in the x and y directions is:

$$\partial_t(HU_x) + \partial_x\left(HU_x^2 + \frac{g_z H^2}{2}\right) + \partial_y(HU_x U_y) = S_{gx} - S_f(R)[n_x] \quad (4)$$

and

$$\partial_t(HU_y) + \partial_x\left(HU_x U_y\right) + \partial_y\left(HU_y^2 + \frac{g_z H^2}{2}\right) = S_{gy} - S_f(R)[n_y] \quad (5)$$

where

$$S_{gx} = g_x H \text{ and } S_{gy} = g_y H \quad (6)$$

are the driving, gravitational accelerations in the x and y directions. The gravitational acceleration vector $\mathbf{g} = (g_x \ g_y \ g_z)$ contains three components which are determined from the coordinates at each point in the model domain.

$S_f(R)$ is the frictional resistance (see below, section 2.2). We do not include momentum losses arising from mass entrainment. $R(x, y, t)$ denotes the mean random kinetic energy of the snow granules and is found from the balance equation:

$$\partial_t(HR) + \partial_x(HRU_x) + \partial_y(HRU_y) = \dot{P} - \dot{D} \quad (7)$$

where $\dot{P}(x, y, t)$ and $\dot{D}(x, y, t)$ represent the production and decay of random kinetic energy of the granular snow mass (Bartelt et al., 2006; Buser and Bartelt, 2008).

2.2 Constitutive Relations

Two frictional models for $S_f(R)$ have been implemented in RAMMS. The Swiss guidelines (Salm et al., 1990), recommend the well-known Voellmy model (Salm, 1993):

$$S_f = \left[\mu(R) g_z H + \frac{g(U_x^2 + U_y^2)}{\xi} \right] \quad (8)$$

with

$$\mu(R) = \mu_0 \text{ and } \dot{P} = \dot{D} = 0.$$

The two model parameters are the Coulomb-friction coefficient μ_0 (a constant independent of R) and the “turbulent” viscous friction ξ (m/s^2). For the energy model, the coefficient of dry friction is dependent on the magnitude of random energy $R(x, y, t)$. Then generation of random energy in the avalanche is proportional to the work done by shear (Buser and Bartelt, 2008a):

$$\dot{P}(x, y, t) = \alpha S_f U \text{ with } S_f U \geq 0 \text{ (always).} \quad (9)$$

It decays by inelastic collisions according to

$$\dot{D}(x, y, t) = \beta(RH) \text{ with } RH \geq 0 \text{ (always).} \quad (10)$$

The value of the constitutive parameter α defines the amount of granule scattering induced by shear tractions within the avalanche flow while the inverse quantity $1/\beta$ can be considered the mean lifetime of the generated random kinetic energy. We have found the generation and dissipation of random energy are seldom in balance: at the front of the avalanche the production term dominates (Bartelt et al., 2007; Buser and Bartelt, 2008a). Only 5% of the total frictional shear work is required to produce random energy, $\alpha = 0.05$. Furthermore, the lifetime of this energy is short $\beta < 0.1 \text{ s}$ leading to the increased shear resistance towards the tail of the avalanche (in comparison to the avalanche front). Therefore, as proposed by Bartelt et al. (2007) Coulomb friction $\mu(R)$ is

$$\frac{d\mu(R)}{dR} = -\frac{\mu(R)}{R_0} \text{ with } \mu(R=0) = \mu_0 \quad (11)$$

where R_0 defines the magnitude of the increase in shear stress as a function of the decrease in random energy density (fluidization) and μ_0 now defines the *static* dry-friction coefficient. Measurements in Vallée de la Sionne show $40 \text{ kJ/m}^3 \leq R_0 \leq 100 \text{ kJ/m}^3$ (Buser and Bartelt, 2008a). This provides μ values in good agreement with snow chute experiments (Platzer et al., 2007).

2.3 Numerical Solution

The governing differential Eqs. 2, 4, 5 and 7 compose a system of non-linear hyperbolic equations which can be written concisely as

$$\partial_t \mathbf{V} + \nabla \cdot \mathbf{F}(\mathbf{V}) = \mathbf{G}(\mathbf{V}) \quad (12)$$

where $\mathbf{V}(x, y, t)$ is a vector containing the four unknown state variables

$$\mathbf{V}^T(x, y, t) = (H \quad HU_x \quad HU_y \quad HR); \quad (13)$$

$\mathbf{F}(\mathbf{V})$ is the flux function. The vector $\mathbf{G}(\mathbf{V})$, located on the right-hand side of Eq. 12, contains source terms (mass entrainment, gravitational accelerations, production of random energy) and sink terms (frictional forces and destruction of random kinetic energy). A finite volume approach is used to solve Eq. 12, requiring the governing equations to be rewritten in integral form. In the finite volume discretization the flux function becomes a surface integral and is discretized using a HLLE (Harten-Lax-van Leer-Einfeldt) scheme. The computational domain is divided into cells of some size, typically between 5m and 10m side length. To guarantee second order convergence in space, a minmod-limited linear reconstruction of the averaged, primary cell quantities is applied. The time-integration is given by a Runge-Kutta-Heun scheme (Kowalski, 2008).

3. MODEL INPUT

Three quantities must be specified to perform a numerical calculation:

- (1) *DEM (Digital Elevation Model)*. DEMs can be generated directly from field measurements (for example, terrestrial or aerial laser scanning data) or obtained directly from a national geo-information center (e.g. SwissTopo in Switzerland). The resolution of the DEM should be between 5m and 25m. Of course, higher resolution DEMs provide more accurate simulations. However, terrain models with a resolution less than 5m do not improve simulation results significantly. Moreover, model calculation time increases significantly and can be prohibitive for high resolution DEMs.
- (2) *Release zone area and fracture height plus snowcover entrainment heights*. Release zones are specified using polygon shapefiles that can be generated within RAMMS. The results from GIS-based terrain analysis can

also be imported into RAMMS. Such a terrain analysis using slope angle, curvature, altitude and vegetation is discussed in Maggioni and Gruber (2003). These procedures are required for large scale hazard mapping applications with RAMMS (Gruber and Bartelt, 2007). Once the release zone areas are defined, the avalanche engineer must provide the fracture height for each release zone. Again, automated procedures are also available within RAMMS that calculate the fracture height based on the Swiss Guidelines (Salm et al., 1990). Snowcover entrainment can be included in the simulations by specifying up to three snow cover layers. This requires defining the density, entrainment coefficient k_i and snowcover layer heights at every point in the model domain. Snowcover heights can also be specified as a function of altitude.

- (3) *Model friction parameters*. Friction parameters can be prescribed manually, or, alternatively, automated procedures have been developed using GIS software. The automated procedures are based on an extensive terrain analysis which classifies terrain features into categories such as open slope/flat terrain/channelled/gully or forested/non-forested (Gruber and Bartelt, 2007). Of course, the friction parameters can be constant over the entire model domain. This is recommended for a first problem analysis.

Geo-referenced maps or aerial photographs can be imported into RAMMS and then superimposed on the computational domain defined by the DEM (Figs. 2). This is an invaluable feature in RAMMS since input specifications can be visualized, controlled and modified if incorrect. Model results are easier to interpret when they are superimposed on maps (Fig. 3 and 4). Although maps are not necessary for a model run, they are very helpful and suggested when using RAMMS.

4. MODEL OUTPUT / VISUALIZATION

A graphical visualization of the numerical calculations is required to evaluate the simulation results. A large effort has been placed into developing user-friendly tools, which allow the quick assessment of runout distances, flow velocities, flow heights, terrain features and entrainment depths.

Output data is written at user-specified dump intervals (usually between 1s and 10s, depending on the problem size). Runtimes vary between 100 and 500 seconds. Thus, there are usually between 10 and 50 calculations steps that are saved on a binary output file. This file is automatically loaded by the graphical interface after completion of the numerical calculations. The output is superimposed on the topography (Figs 2 and 3). The topography can be depicted on a plane in two-dimensions or fully in three-dimensions (Fig. 3 and 4). Both two- and three-dimensional depictions can be zoomed, shifted and rotated in order to find the best perspective. The superimposed output can then be visualized at each step, or animated over all the saved dump steps. The numerical values are written in a window below the main graphics window. It is continuously updated when the mouse is moved from location to location in the main window. By clicking at a particular location XY-time plots (e.g. the time-evolution of the flow height) are displayed in a separate window.

Another important feature in RAMMS is the animated display of the eroded snowcover. Color profiles of snowcover layer heights allow a quick determination of where snow is being entrained in the avalanche (front, tail, etc.) at which track sections (gullies, runout zones, etc).

Other built-in output functions include:

- Defining one-dimensional line profiles or flow sections and then depicting/animating a state-variable on this cross-section.
- Flowing mass reports defining the total volume of snow moving at any given time. This is often used to determine when the avalanche has actually stopped. The entire mass balance at any given time can then be analysed. This helps to define proper snow cover entrainment rates.
- Plots showing the deposition/flow heights as a function of slope angle. Since this information is often available from laser scanning studies, this helps determine the correctness of the simulation results.

Finally, results can be exported as ESRI shapefiles and compared in ArcGIS with measured data. ESRI shapefiles can also be imported into RAMMS. Additionally, GIF/TIFF files, GIF animations and ASCII files can be exported and used in engineering reports. A useful gimmick is the possibility to export simulation results to Google Earth.

5. EXAMPLE SIMULATION

On the 23rd of April 2008, a large wet snow avalanche occurred at Gatschiefer, near Monbiel/Klosters, Canton Grisons (Fig. 1). An early Spring snow storm that started on the evening of the 21st of April deposited some 80cm to 120cm of new snow above 2200 m within 24 hours. The avalanche occurred during the late afternoon at around 16:00. Luckily, a local bus driver filmed the event with his cell phone and clear weather immediately after the event allowed the identification of a large release zone. However, rain quickly set in preventing further observations. The velocity of the avalanche was estimated from the video to be 5 m/s over the last 750 m runout distance. The avalanche struck a deflecting dam, overflowing the dam slightly at its downward end. The avalanche entered the forest opposite the dam and in the deposition zone and many trees were overturned by the slow moving mass. Deposits on the dam (and the video images) indicated the flow heights to be higher than 5m. Aerial laser scanning was performed on the 26th of April, after the rain stopped (it rained between the 23rd and 25th).

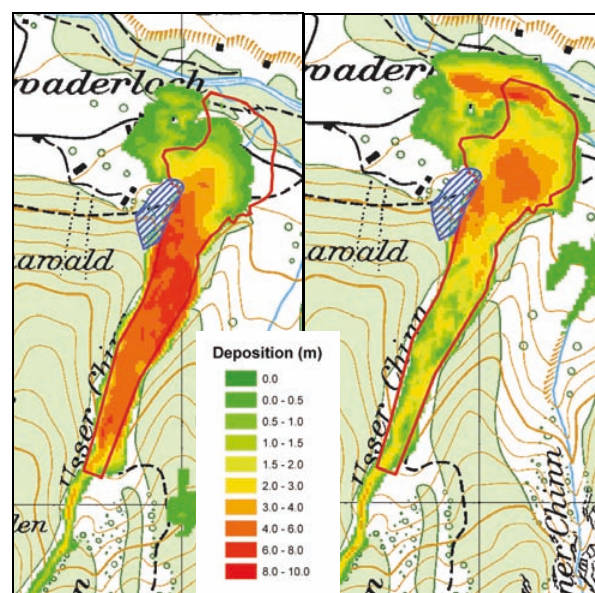


Figure 2: Calculated depositions using the Voellmy-model (left) and R-energy model (right) and comparison to laser scanning measurements (red outline). Note the difference in predicted distribution. The dam is shaded in blue.

The maximum deposition heights in the runout zone were found to be close to 9m; however, deposition heights at the avalanche front were typically between 5m and 6m. Deposits

behind the dam were on the order of 2m. The avalanche did not reach the river Landquart, but it did descend the steep banks. Here the deposition heights were large (approx 10m). From the laser scanning data we estimated the total deposition volume to be between 410'000 m³ and 480'000 m³, covering an area of 115'000 m². Granulometry studies of the deposits indicated mean granule size of 10cm; however, intermixed in the granular deposits we found large snow clods (diameters greater than 50cm) and woody debris. At several locations at the tail of the deposits the ground was exposed, the snow clods covered with dirt, indicating significant basal shearing at the bottom of the avalanche.

The first problem we confronted with the simulation of the Gatschiefer avalanche was the DEM. During an extreme rainfall period in 2005, the banks of the river Landquart were eroded changing the course of the river and the river bank terrain. We used a pre-2005 DEM, realizing that final reaches of the avalanche motion, the rapid descent down the steep river banks, might not be modeled exactly. We specified two release zones, based on the post-event photographs (Fig. 1). The first release zone was in the steep terrain between 2100 m and 2300 m; while the second release zone, smaller in size, was located between 1900 m and 2000 m. The total area of both release zones was 220'000 m². The fracture height of both release zones was set to 1m, in accordance with the meteorological observations.

We simulated the Gatschiefer avalanche with entrainment, specifying one snow layer $h_1 = 70$ cm with a density of $\rho_1 = 200$ kg/m³ (moist snow). We estimated the return period of this avalanche to be $T \approx 30$ years. The unit entrainment rate was chosen to be $k_1 = 0.2$. Both Voellmy-fluid and R-energy relations were applied to model the event (Fig. 2). The Voellmy-model used variable wet-snow avalanche parameters automatically defined within RAMMS (see Gruber and Bartelt, 2007). The R-energy model parameters were held constant over the entire model domain: $\mu_0 = 0.2$; $\xi = 250$ m²/s; $\alpha = 0.05$; $\beta = 0.75$ s⁻¹.

Both models predicted that beyond the dam the avalanche would spread to the left — inundating a small settlement of farm buildings (Fig. 2). The avalanche did in fact flow in this direction, but stopped before the numerical predictions. The R-energy model predicted the proper reach of the avalanche and a more realistic distribution of deposition heights; the largest

deposition heights being beyond the dam, as in reality. The calculated deposition heights are furthermore in good agreement with the laser scanning measurements. The predicted runout distances using the Voellmy-fluid model are somewhat too short. Furthermore, most of the mass is deposited in the channel above the dam, which is not in agreement with the measurements. The calculated deposition volumes of 435'000 m³ (R-energy) and 450'000 m³ (Voellmy) are well within the range of the laser scanning measurements. The Voellmy-model entrained more mass because the calculated velocities in the runout zone were larger. The R-energy model predicts velocities less than 5 m/s in the runout zone (Fig. 3), again in good agreement with the bus driver's video.

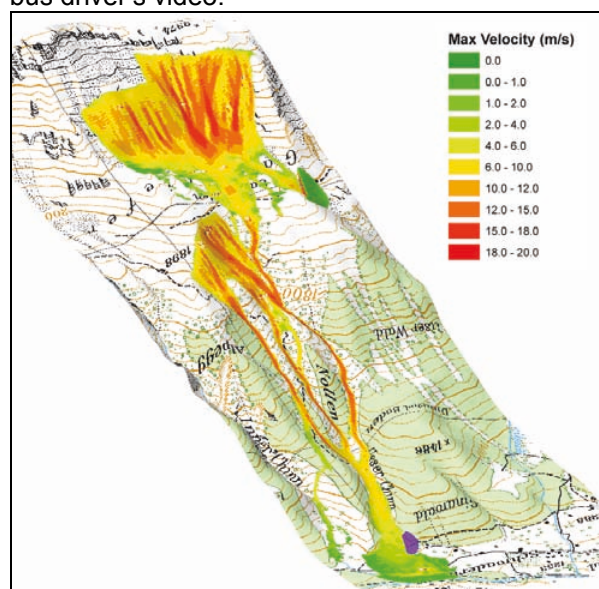


Figure 3: Maximum flow velocities. In the runout zone the velocities are lower than 5m/s.

The simulations showed that the avalanche dam, constructed after the avalanche winter of 1999 to protect several houses, had a large influence on the flow, deflecting it towards the river. The simulated avalanche did not overrun the dam, in good agreement with the observations.

CONCLUSIONS

RAMMS is a powerful tool for predicting avalanche runout and flow velocities in three-dimensional terrain. The tool was designed to contain state-of-the-art physics coupled with easy to use input and output features. RAMMS can simulate real avalanches; however, more model testing remains to find the limits of its application.

The inclusion of snowcover entrainment in RAMMS has greatly improved the ability of avalanche dynamics models to predict avalanche flow and deposition heights. We found $0.05 \leq k_i \leq 0.2$ provided realistic peak

entrainment rates of $500 \text{ kg/m}^2 \text{ s}$, which have been observed in Vallée de la Sionne (Sovilla et al., 2006). The multilayer snowcover model allows us to simulate different entrainment mechanisms: large k_i values corresponding to frontal plowing while low values model basal erosion. In future we would like to add a limit stress or fracture toughness (Cherepanov and Esparragoza, 2008) to control the initiation of the entrainment process. This would allow avalanche motion without entrainment when the limit stress (or fracture toughness) of the layer is not reached. However, at present, we simply do not know how to quantify the chaotic stress state that exists at the avalanche front or bottom, making the formulation of a stress-based or fracture entrainment model both difficult to implement and verify.

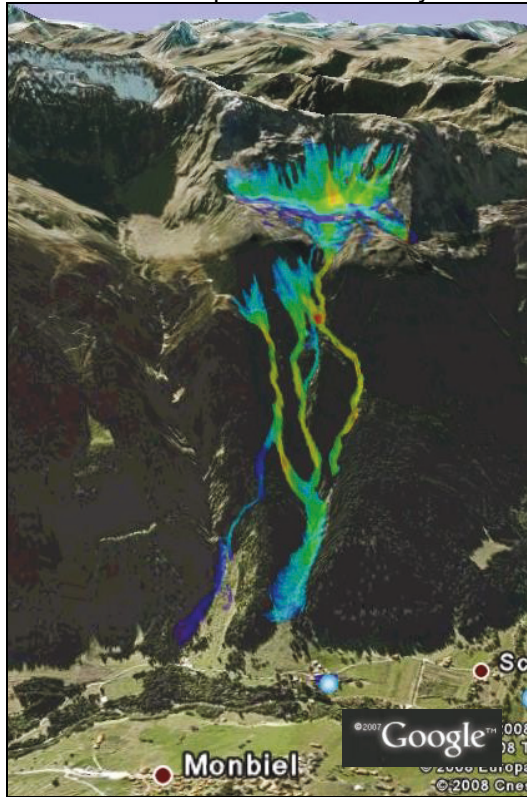


Figure 4: Maximum entrainment rates exported to Google-Earth. Printed with permission of Google-Earth.

In the first version of RAMMS, the system of governing equations was solved using first-order

schemes. We found this to be inadequate, since the calculated avalanches spread too widely in open, unchannelled runout zones. We subsequently introduced second-order schemes. The second order schemes not only improved flow width predictions but also entrainment calculations. If the avalanche spreads too widely, too much mass is additionally entrained in the avalanche leading to a false avalanche mass balance. Therefore, the second order schemes not only improved the numerical accuracy of the computations, but also made it easier to control entrainment processes.

The underlying principle behind the energy model within RAMMS is that shear deformations within the flow produce random kinetic energy. The generation rate of the random energy is equal to the work done by the viscous shearing work -- minus the energy dissipated to heat. Therefore, there is a transfer of energy within the avalanche from the mean flow to the random motion of the snow clods. The increase in random energy coincides with a reduction of the viscous shear stress. However, the amount of random kinetic energy depends on the inelastic collisional interactions between the snow/ice granules. It appears that the random energy is produced at the avalanche front, but the collisional interactions cause it to decay towards the avalanche tail. In fact, measurements at the Vallée de la Sionne test site (as well as the simulations of the Gatschiefer avalanche) show that the lifetime of random kinetic energy in an avalanche is less than the time it takes an avalanche to pass the measurement pylon, $1/\beta \leq 10 \text{ s}$ (say). Therefore, the shear stress at the avalanche front is smaller in comparison to the tail. Thus, the energy model in RAMMS allows us to simulate avalanches that deposit mass, or starve (Bartelt et al., 2007) on steep slopes. This is an improvement over the conventional Voellmy-model, where such problems had to be solved by ad-hoc manipulations of the magnitude of μ as a function of avalanche size.

Interestingly, some random energy might even escape the front or top surface of the flowing avalanche. When this happens, the random energy loses its non-directional character. In the absence of collisions (dilute flows), the random energy takes on a directional and subsequently dangerous quality. In future we hope to include energy fluxes across the mass boundaries of a flowing avalanche to simulate saltation layers and perhaps even the initiation of powder snow avalanches.

7. ACKNOWLEDGEMENTS

The authors thank Arthur Sandri and Christian Wilhelm from the Federal Office of the Environment (FOEN/BAFU) and the Government of Grisons for financing the aerial laser scanning of the Gatschiefer avalanche.

8. REFERENCES

Bartelt, P., B. Salm and U. Gruber, 1999. Calculating dense-snow avalanche runout using a Voellmy-fluid model with active/passive longitudinal straining. *J. of Glaciol.*, 45(150), 242-254.

Bartelt, P., O. Buser and K. Platzter, 2006. Fluctuation-dissipation relations for granular snow avalanches, *J. Glaciol.*, 52(179), 631 -- 643.

Bartelt, P., O. Buser and K. Platzter, 2007. Starving avalanches: Frictional mechanisms at the tails of finite-sized mass movements, *Geophysical Research Letters*, 34(20), L20407.

Buser, O. and P. Bartelt, 2008a. The production and decay of random energy in granular snow avalanches, *J. Glaciol.*, submitted for publication.

Buser, O. and P. Bartelt, 2008b. Energy Fluxes in Snow Avalanches, in the Proceedings of the Russian Glaciology Meeting, Siberia, September, 2008.

Cherepanov G and I. Esparragoza, 2008. A fracture entrainment model for snow avalanches, *J. of Glaciol.* 53(184), 182-188.

Christen, M., Bartelt, P. & Gruber, U. 2002. AVAL-1D: An avalanche dynamics program for the practice. Proceedings of the International Congress Interpraevent 2002 in the Pacific Rim, 14-18 October 2002, Matsumoto, Japan. Vol. 2, pp. 715-725.

Christen, M., P. Bartelt and U. Gruber, 2007. Modelling Avalanches. *GEOconnexion International* 6, 4: 38-39.

Gruber, U. and P. Bartelt, 2007. Snow avalanche hazard modelling of large areas using shallow water numerical methods and GIS, *Environmental modelling & software*, 22(10), 1472-1481.

Kern, M., F. Tiefenbacher and J. McElwaine, 2004. The rheology of snow in large chute flows, *Cold regions science and technology*, 39(2-3), 181-192.

Kern, M., P. Bartelt, B. Sovilla and O. Buser, 2008. Measured shear rates in large dry and wet snow avalanches, *J. Glaciol.*, accepted for publication.

Kowalski, J. 2008. Two-phase debris flow modeling. Dissertation, Seminar for Applied Mathematics, SAM, ETH Zürich.

Maggioni, M and U. Gruber, 2003. The influence of topographic parameters on avalanche release and frequency. *Cold regions science and technology*, 37(3), 407-419.

Platzter, K., P. Bartelt and M. Kern, 2007. Measurements of dense snow avalanche basal shear to normal stress ratios (S/N), *Geophysical Research Letters*, 34(7), L07501.
Salm, B. 1993. Flow, flow transition and runout distances of flowing avalanches. *Ann. Glaciol.*, 18, 221 - 226.

Salm, B., A. Burkard and H. Gubler, 1990. Berechnung von Fliesslawinen: eine Anleitung für Praktiker mit Beispielen. Eidg. Inst. Schnee- und Lawinenforschung. Mitteilung 47.

Sovilla, B., P. Burlando and P. Bartelt, 2006. Field experiments and numerical modelling of mass entrainment in snow avalanches, *J. Geophys. Res.*, 111(F3), F03007. doi:10.1029/2005JF000391).

Sovilla, B., M. Schaer, M. Kern and P. Bartelt, 2007. Impact pressures and flow regimes in dense snow avalanches observed at the Vallée de la Sionne test site, *J. Geophys. Res.*, doi:10.1029/2006JF000688.